Looking for the sponge loop: analyses of detritus on a Caribbean forereef using stable isotope and eDNA metabarcoding techniques

Lauren K Olinger [Corresp., 1, 2], **Beverly McClenaghan** [3], **Mehrdad Hajibabaei** [3, 4], **Nicole Fahner** [3], **Lesley Berghuis** [3], **Hoda Rajabi** [3], **Patrick Erwin** [2], **Chad S Lane** [5], **Joseph R Pawlik** [2]

[1] Center for Marine and Environmental Studies, University of the Virgin Islands, St Thomas, Virgin Islands, U.S. Virgin Islands

[2] Department of Biology and Marine Biology, University of North Carolina Wilmington, Wilmington, North Carolina, United States

[3] eDNAtec Inc., Newfoundland and Labrador, St. John's, Canada

[4] Department of Integrative Biology, University of Guelph, Guelph, Ontario, Canada

[5] Department of Earth and Ocean Sciences, University of North Carolina Wilmington, Wilmington, North Carolina, United States

Corresponding Author: Lauren K Olinger
Email address: l.olinger12993@gmail.com

Coral reefs are biodiverse ecosystems that rely on trophodynamic transfers from primary producers to consumers through the detrital pathway. However, little is known about the composition of detritus on Caribbean coral reefs. Some theorize that cryptic sponges produce large quantities of detritus on coral reefs as part of a hypothesized sponge loop. In this study, we collected samples of detritus in the epilithic algal matrix (EAM) and samples from potential sources of detritus over two seasons from the forereef at Carrie Bow Cay. We utilized stable isotope analyses and eDNA metabarcoding to determine the composition of the detritus. The EAM detritus was derived from a variety of benthic and pelagic sources, with primary producers (micro- and macroalgae) as major contributors and metazoans (Arthropoda, Porifera, Cnidaria, Mollusca) as minor contributors. None of the cryptic sponge species that reportedly produce detritus were present in EAM detritus, despite their relative abundance in the reef interstices. The cnidarian signature in EAM detritus was dominated by octocorals, with a scarcity of hard corals. The composition of detritus also varied seasonally. The negligible contribution of sponges to reef detritus contrasts with the detrital pathway originally proposed in the sponge loop hypothesis. The findings indicate a mix of pelagic and benthic sources in the calmer summer and primarily benthic sources in the more turbulent spring.

Looking for the sponge loop: Analyses of detritus on a Caribbean forereef using stable isotope and eDNA metabarcoding techniques

Lauren K. Olinger[1,2]*, Beverly McClenaghan[3], Mehrdad Hajibabaei[3,4], Nicole Fahner[3], Lesley Berghuis[3], Hoda Rajabi[3], Patrick Erwin[1], Chad S. Lane[5], Joseph R. Pawlik[1]

[1] Department of Biology and Marine Biology, University of North Carolina Wilmington, Wilmington, NC, USA

[2] Center for Marine and Environmental Studies, University of the Virgin Islands, Saint Thomas, VI, USA

[3] Centre for Environmental Genomics Applications, eDNAtec Inc., Newfoundland and Labrador, St. John's, Canada

[4] Department of Integrative Biology, University of Guelph, Guelph, ON, Canada

[5] Department of Earth and Ocean Sciences, University of North Carolina Wilmington, Wilmington, NC, USA

Corresponding Author:

Lauren Olinger

2 John Brewers Bay, St. Thomas, VI, 00802, USA

Email address: l.olinger12993@gmail.com

Abstract

Coral reefs are biodiverse ecosystems that rely on trophodynamic transfers from primary producers to consumers through the detrital pathway. However, little is known about the composition of detritus on Caribbean coral reefs. Some theorize that cryptic sponges produce large quantities of detritus on coral reefs as part of a hypothesized sponge loop. In this study, we collected samples of detritus in the epilithic algal matrix (EAM) and samples from potential sources of detritus over two seasons from the forereef at Carrie Bow Cay. We utilized stable isotope analyses and eDNA metabarcoding to determine the composition of the detritus. The EAM detritus was derived from a variety of benthic and pelagic sources, with primary producers (micro- and macroalgae) as major contributors and metazoans (Arthropoda, Porifera, Cnidaria, Mollusca) as minor contributors. None of the cryptic sponge species that reportedly produce detritus were present in EAM detritus, despite their relative abundance in the reef interstices. The cnidarian signature in EAM detritus was dominated by octocorals, with a scarcity of hard corals. The composition of detritus also varied seasonally. The negligible contribution of sponges to reef detritus contrasts with the detrital pathway originally proposed in the sponge loop hypothesis. The findings indicate a mix of pelagic and benthic sources in the calmer summer and primarily benthic sources in the more turbulent spring.

Key words – detritus, coral reef, trophodynamics, Porifera

Introduction

Coral reefs are among the most biodiverse marine ecosystems despite occurring in oligotrophic tropical waters (Darwin and Bonney 1896). The paradoxical survival of coral reefs in such marine deserts is made possible by high primary productivity and efficient nutrient cycles (Mumby and Steneck 2018). However, the survival of coral reefs is at risk due to human-driven climate change, diseases, overfishing, and other stressors (Hughes 1994; Hoegh-Guldberg et al. 2007). These stressors are driving the replacement of reef-building corals by non-reef building organisms, such as algae, sponges, and benthic cyanobacterial mats (BCM), reducing reef complexity, accretion, water quality, and overall habitat value for higher trophic levels (Done 1992; Aronson et al. 2002; Fabricius 2005; Norström et al. 2009; de Bakker et al. 2017). Changes to benthic communities also cause cascading effects to the nutrient cycles on which these ecosystems rely, including how energy is transferred from primary producers to higher trophic levels through the detrital pathway (Begon et al. 1986; Johnson et al. 1995; Wilson et al. 2003).

Detritus is a protein- and amino acid-rich mixture (Wilson 2000; Crossman et al. 2001) of non-living organic matter derived from non-fossil living sources and living organic matter from heterotrophic and autotrophic microbes (Begon et al. 1986; Wilson et al. 2003). The combination of detritus and inorganic carbonates and silicates forms benthic particulates on coral reefs (Tebbett and Bellwood 2019). The accumulation of detritus-laden particulates in the turf-forming algae that covers dead coral surfaces is collectively known as the epilithic algal matrix (EAM), and this amalgamation of nutritious detritus and algae is an important food resource for many fish and invertebrate detritivores (Hatcher 1983; Purcell and Bellwood 2001; Wilson et al. 2003; Kramer et al. 2012).

Detrital organic matter on coral reefs is derived from a variety of autochthonous and allochthonous benthic and pelagic sources. Micro- and macro-algae are major sources of detritus that accumulate on the benthos following mechanical breakdown by physical forces or through grazing (Hatcher 1983; Alongi 1988; Wilson et al. 2003). Algae can also produce detritus indirectly by generating photosynthate, forms of dissolved organic carbon (DOC) that can aggregate into non-cellular amorphic detritus by adsorbing to carbonate sediments or spontaneously forming polymer gels (Otsuki and Wetzel 1973; Chin et al. 1998; Wilson et al. 2003). Another source of detritus is bacteria (Tebbett and Bellwood 2019) that can form biofilms and act as nucleation sites for DOC aggregation, and heterotrophic bacteria can consume detritus and mediate its transformation to a form that can be consumed by metazoans (Biddanda 1985; Alongi 1988; Wilson et al. 2003). Benthic cyanobacterial mats (BCM) are also becoming more abundant on Caribbean coral reefs (de Bakker et al. 2017) and may be similar to benthic macroalgae with respect to their contribution to detritus, either directly through mechanical breakdown following physical detachment from the reef, or indirectly through production of large quantities DOC (Brocke et al. 2015) that may aggregate and build up in the EAM.

Detritus may also be derived from the shedding of mucus or cells by benthic metazoans, namely corals and sponges. Coral mucus has long been considered an important source of detritus on coral reefs (Gottfried and Roman 1983). Sponges have more recently been implicated in detritus production, and sponge conversion of DOC to detritus may be an important mechanism recycling carbon back to the benthos before it can escape the reef, thereby aiding in tight carbon cycles that ensure reef survival under oligotrophic conditions (de Goeij et al. 2013). This conversion of DOC to detritus is the theorized sponge loop, named after the similar microbial loop which describes the return of DOC back into the grazing food web via predation

on free-living microbes by protists (Azam et al. 1983). Since its proposal, the sponge loop hypothesis has been widely cited and has been featured in undergraduate marine biology textbooks (Levinton, 2021).

The sponge loop hypothesis was originally proposed based on experiments with the thinly encrusting cryptic sponge *Halisarca caerulea,* and detritus production has been reported for *H. caerulea* and three other cryptic sponge species (*Haliclona vansoesti*, *Chondrilla caribensis*, and *Scopalina ruetzleri*) through rapid cellular proliferation and choanocyte turnover associated with space-limitation and restricted growth (de Goeij et al. 2013). Emergent sponge species that grow above the reef were not found to be net producers of detritus and instead were suggested to return DOM to the benthos as sponge biomass (McMurray et al. 2018). More recently, some emergent sponge species, including the Caribbean species *Aplysina archeri,* were observed "sneezing" mucus and particulates from near their incurrent ostia (Kornder et al. 2022), but it is not yet clear if this is a method of detritus production analogous to that of cryptic sponge species or whether this mechanism is common across the emergent sponge fauna. The discovery of the microbial loop accounted for a large fraction of missing oceanic carbon (Fenchel 2008), but it is unclear whether the carbon transformation mediated by the sponge loop is as important a pathway.

Detritus collected from a forereef off Palmyra Atoll showed abundant pelagic inputs (Max et al. 2013). Studies such as those conducted on the Palmyra Atoll by Max et al. (2013) used stable isotope analyses (SIA) to determine the sources contributing to benthic detritus. SIA is a popular technique for tracing energy flow through ecosystems, and it is based on the discrimination against heavier isotopes in metabolic processes, which separates organisms from different trophic levels along axes of $^{15}N/^{14}N$ and separates organisms with different types of

primary productivity and carbon sources along axes of $^{13}C/^{12}C$ (Post 2002; Michener and Kaufman 2007; Middelburg 2014; Zapata-Hernández et al. 2021). SIA has been relatively underused to explore trophodynamics on coral reefs (Greenwood et al. 2010).

While popular, SIA is not able to discern between species with similar trophic levels and carbon-fixing pathways. This limitation can be resolved with supplemental collection and metabarcoding of environmental DNA (eDNA) samples, an increasingly popular approach for characterizing biodiversity that does not require collection of whole biological specimens and instead relies on recovery and analysis of DNA from the physical environment in which they live (e.g., water, soil, sediment; Thomsen and Willerslev 2015). This eDNA is released from organisms through various mechanisms, including cell shedding and the excretion of various bodily fluids and feces, and it can be isolated, amplified, and sequenced using high-throughput genomic sequencing platforms and then screened against publicly available databases (e.g., GenBank) to assign taxonomy to the organisms contributing to that environmental sample (Baird and Hajibabaei 2012; Taberlet et al. 2012; Thomsen and Willerslev 2015). Analyses of eDNA have been used to quantify biodiversity (Thomsen and Willerslev 2015), determine species diets (Boyi et al. 2022), and identify elusive species (McClenaghan et al. 2020). Analyses of eDNA can also complement SIA-based estimations of source contributions to organic matter resources, such as detritus. A similar SIA/eDNA approach was recently used to quantify the relative contributions of different sources to sediment organic carbon in seagrass meadows (Reef et al. 2017).

In this study, samples of reef detritus and samples from potential sources of detritus, including from organisms and from areas where detritus may originate (e.g., water column, fish feces) were collected from a Caribbean forereef over two seasons (July 2018 and March 2019).

Stable isotope and eDNA metabarcoding analyses were applied to the samples to explore the composition of detritus, with a particular focus on sponges to test claims that sponges are major sources of detritus on Caribbean coral reefs (de Goeij et al. 2013).

Materials & Methods

Sample collection

Samples were collected in July 2018 and March 2019 from the forereef near the Smithsonian field station at Carrie Bow Cay, Belize. Carrie Bow Cay is situated on the Mesoamerican Barrier Reef, approximately 22 km from the city of Dangriga on mainland Belize. The characteristic spur-and-groove formation of the forereef at 15-20 m depth is an *Orbicella annulari*s framework with abundant octocorals, sponges, and algae. The forereef location (16°48'10.6"N, 88°4'43.9"W) approximately 500 m northeast of the island of Carrie Bow Cay drops off steeply at the outer ridge less than 100 m to the east. Cuts to the north and south of the island and reef isolate the complex from the rest of the Mesoamerican barrier reef and expose the area to currents that flow through the channels, including waters from the open ocean and from the shoreward lagoon with large mangrove islands and seagrass beds nearby. The reef complex at Carrie Bow Cay has been extensively studied since its founding as a research site by scientists in 1972 (Rützler and Macintyre 1982). Field experiments were approved by the Belize Fisheries Department (permit number 00023-18).

Two categories of samples were collected from the forereef: detritus and detritus sources, where the latter refers to organisms or materials that may be contributing to detritus. Samples also encompassed either tissues or composites, where tissues refer to organic material deliberately collected from a living organism and composites refer to organic remnants of

multiple organisms that had been previously deposited to the water column or benthos as particulates or feces.

Two types of detritus were collected: detritus from the epilithic algal matrix (EAM detritus) and detritus from plastic trays placed under reef overhangs (tray detritus). Seven types of source samples were collected: algae tissue, benthic cyanobacterial mat (BCM) tissue, feces from two species of herbivorous fish, feces from two species of spongivorous fish, tissues of three emergent sponge species, tissues of three cryptic sponge species, and water column particulates from sediment traps (Table 1).

EAM and tray detritus

Detrital material was suctioned from a 25 cm^2 area of epilithic algal matrix (EAM) using 50 ml polypropylene syringes. EAM samples (2018 n = 5, 2019 n = 11) were collected at least 10 m apart and from flat patches of dead rock covered with closely cropped turf and devoid of pits (Purcell and Bellwood 2001). In 2019, trays (white plastic bins with dimensions 40 x 31.8 x 15.2 cm; n = 6) were deployed under reef overhangs to target detrital outfall from organisms, including cryptic sponges. After 72 h, the particulates and detritus that had accumulated in the trays were suctioned up using 50 ml polypropylene syringes. Syringes of EAM and tray detritus were transported back to the lab at Carrie Bow Cay, where their contents were filtered through a 150 μm mesh to isolate the smaller size fraction targeted by detritivores (Wilson et al. 2003). The mixture was divided, with approximately 5 ml transferred to a microcentrifuge tube with 0.5 ml ethanol and the remaining filtered onto a 0.7 μm filter (Watson GFF), and both samples were stored at -20°C.

178 *Tissue samples*

179 The tissues of organisms that are abundant and possible contributors to reef detritus were
180 collected at the same location and time (July 2018, March 2019) as detritus collections. Divers
181 sought out different individuals or patches of each targeted organism; species were visually
182 identified on site, and identifications were later validated with genetic sequence data for all but
183 the most conspicuous organisms (*Aplysina cauliformis*, *Niphates digitalis*, and *Halimeda* sp).
184 When collecting the tissue samples, the sample quantity and collection method varied by species.
185 The algae and benthic cyanobacterial mat (BCM) tissues were collected in handfuls, using snips
186 to separate algae or bacterial tissues from each source patch, and transferred to the lab at Carrie
187 Bow Cay in plastic bags. The tissues of emergent sponge species *Xestospongia muta, A.*
188 *cauliformis,* and *N. digitalis* were collected with a dive knife or cork borer (1 cm diameter), and
189 clean pieces of tissue (approximately 8 cm^3 or 2 cm cylinders) were transported to the lab at
190 Carrie Bow Cay in plastic bags. Tissues of cryptic sponge species *Chondrilla* sp., *Halisarca*
191 *caerulea*, and *Scopalina ruetzleri* were removed from rock using a scalpel blade, producing
192 tissue samples that were approximately 4 cm^2 and 1-2 mm thick. All tissue samples were sealed
193 at depth in plastic bags and transported back to the lab, where a subsample of tissue (< 1 cm^3)
194 from each organism was transferred to a microcentrifuge tube, rinsed twice with ethanol, and
195 stored in 0.5 ml ethanol at -20°C. The plastic bag with the remaining tissue sample was squeezed
196 of excess water, resealed, and frozen at -20°C.

197 *Feces samples*

198 Feces of two herbivorous fish species (*Acanthurus bahianus, Acanthurus coeruleus*) and
199 two spongivorous fish species (*Holacanthus ciliaris, Pomacanthus paru*) were also collected.
200 For these samples, divers observed fish, and when the fish was seen defecating, the diver used a

turkey baster to collect the feces before it touched the benthos. The contents of the turkey baster were transferred to a plastic bag, sealed at depth, and transported back to the lab. The mixture was divided, with approximately 5 ml transferred to a microcentrifuge tube with 0.5 ml ethanol and the remaining filtered onto a 0.7 µm filter (Watson GFF), and both samples were stored at -20°C.

Sediment trap samples

Sediment traps made of PVC pipe with diameter of 7.6 cm and length of 30.5 cm (4:1 aspect ratio) were deployed on the reef for 72 h to capture water column particulates that may be contributing to detritus. While seawater samples would have been a more representative sample of pelagic contributions to reef detritus, this was not feasible due to the volume of water (>> 4 L) required for stable isotope analyses. Traps (2018 n = 5; 2019 n = 15; Table 1) were deployed at least 10 m apart on the reef and affixed with cable ties to a metal stake that had been securely driven into dead coral heads. After 72 h, plastic bags and rubber bands were used to seal sediment traps at depth before being transported to the lab at Carrie Bow Cay for processing. The mixture was divided, with approximately 5 ml transferred to a microcentrifuge tube with 0.5 ml ethanol and the remaining filtered onto a 0.7 µm filter (Watson GFF), and both samples were stored at -20°C.

Stable isotope analyses

Samples were transported on ice to University of North Carolina Wilmington (UNCW), where tissue samples and filters containing composite samples were transferred to combusted scintillation vials and lyophilized for 24 h. Dried tissue samples were ground into a powder using a mortar and pestle, and the powder was returned to the scintillation vials. Filters were cut in half using a scalpel. One half of each filter and approximately 10 mg of each tissue sample was

transferred to a second combusted vials for acidification by exposure to vapors of 12 M HCl for 24 h. Acidified samples were then placed on a 60°C hotplate for 48 h to boil off remaining HCl. Each of the non-acidified and acidified filter halves were halved again, and the quarter filter segments were transferred to foil capsules. For each non-acidified and acidified tissue sample, an ultra-microbalance was used to precisely measure (within 5%) a target weight of sample into foil capsules. Target weights varied from 2 mg for *Dictyota* to 7 mg for *Lobophora*, and 4 mg for all other sampled species (six sponge species, BCM, and *Halimeda*).

Non-acidified and acidified samples were analyzed for nitrogen and carbon stable isotope compositions, respectively, using a Costech 4010 Elemental Analyzer interfaced with a Thermo Delta V Plus stable isotope mass spectrometer at UNCW. Isotopic results are expressed in standard delta (δ) units calculated as follows: $\delta^{13}C$ or $\delta^{15}N$ (‰) = $1000[(R_{sample} / R_{standard}) - 1]$, where R_{sample} and $R_{standard}$ are the $^{13}C/^{12}C$ or $^{15}N/^{14}N$ ratios of samples and standards, respectively. Within-run standard deviations of $\delta^{13}C$ and $\delta^{15}N$ were < 0.3‰ across repeated analyses of USGS 40 and USGS 41a glutamic acid standards (average = 0.2‰, min = 0.1‰). A total of 8 samples from 2019 were omitted from analyses due to insufficient acidification leading to remnant inorganic carbon species, as determined by $\delta^{13}C$ values that exceeded -10 (Schidlowski 2001). For fish feces samples collected in 2019, the stable isotope composition of three feces samples (n = 2 from herbivore *Acanthurus bahianus* and n = 1 from spongivore *Holocanthus ciliarus*) were not measured due to insufficient material on the filter, but these samples were subjected to genetic sequencing.

Metabarcoding analyses

The samples stored in microcentrifuge tubes in ethanol were shipped to the Center for Environmental Genomics Analysis (CEGA) for sequencing in 2019. CEGA designed and

optimized a fully custom eDNA analysis. DNA extraction methods were optimized for each sample type to maximize DNA recovery, and DNA was extracted from all samples using the optimized protocols. Three DNA markers partially covering three genetic regions (cytochrome *c* oxidase I, 18S rRNA, 16S rRNA) were amplified from each sample using PCR (Table S1-2). These markers were chosen to provide comprehensive detection of metazoans, algae, and cyanobacteria. Negative controls were added during extraction and PCR steps and carried through to sequencing. The three amplicons from each sample were sequenced on an Illumina NovaSeq 6000 instrument with a target minimum sequencing depth of 250,000 sequences per sample per marker. See Supplemental Information for detailed DNA extraction and library preparation procedures. Raw sequence reads are available in NCBI's sequence read archive under project PRJNA965826.

After DNA sequencing, base calling and demultiplexing were performed using Illumina's *bcl2fastq* software (v2.20) and primers were trimmed from sequences using *cutadapt* (v2.8; Martin 2011). Using *DADA2* (v1.14; Callahan et al. 2016) with default parameters, sequences were filtered for quality and length and then denoised to create exact sequence variants (ESVs), each of which represent a unique sequence from the sample. ESVs were assigned taxonomy using NCBIs's *blastn* tool (v2.11; Altschul et al. 1990) and the *nt* database (downloaded November 25, 2020) with an e-value cut-off of 0.001. The taxonomy presented here matches the naming conventions used in NCBI's taxonomy database and was assigned based on a sequence similarity score (the product of the percent sequence similarity and the percent query coverage). The minimum scores for taxonomic assignment at each level were as follows: phylum at 85%, class and order at 90%, family at 95%, genus at 98%, and species at 99%. The results from all markers were consolidated to create the taxonomic lists. Taxonomic identifications were verified

against the World Register of Marine Species (WoRMs), Global Biodiversity Information Facility (GBIF), and the Encyclopedia of Life (EOL) to ensure that spurious matches resulting from poor reference database coverage were not included in the list. As standard practice, ESVs assigned to humans, common insect pests (e.g., mosquitos, beetles), and food (e.g., chicken) were removed from the sample data. Sequencing results from the negative controls generated during lab processing were screened for contamination, and any ESVs detected in the negative controls were removed from the associated samples. No ESVs were amplified from negative controls that were also detected in associated samples and could be assigned taxonomy based on the selection criteria described above.

Data analyses

Bayesian stable isotope mixing models (R package SIMMR; Parnell 2019) were used for the two tracer isotopes (^{13}C, ^{15}N). For July 2018 samples, the mixing model was parameterized using the EAM detritus as the mixture and 11 sources: algae tissue (combined *Dictyota* and *Lobophora*), BCM tissue, herbivore feces (combined *A. bahianus* and *A. coeruleus*), spongivore feces (*H. ciliaris*), emergent sponge tissue from three species (*Aplysina cauliformis, Niphates digitalis*, and *Xestospongia muta*), cryptic sponge tissue from three species (*Chondrilla* sp, *Halisarca* sp., *Scopalina ruetzleri*), and sediment trap samples. The algae tissue types were initially pooled as a single source because of the large overlap between the two species in isotopic space, and the herbivore feces were combined for the same reason. However, sponge species were retained as separate sources in the mixing model due to little overlap in isotopic space. For March 2019 samples, two mixing models were parameterized (one each for suction and tray detritus) with the same number and type of sources as the 2018 samples, with the addition of *Halimeda* sp. to the combined algae tissue category and feces of *P. paru* to the

combined spongivore feces category. Each model was run with 10000 iterations, thinned by 10, and with an initial discard of the first 1000 iterations. We examined correlations among the posterior distributions in each model to assess the ability of the model to distinguish between different sources, pooled highly correlated sources, and re-ran the model with the pooled sources, keeping other settings the same.

For genetic sequencing data, ESV identifications were tabulated across sample types and years to determine the frequency of occurrence at the level of taxonomic phyla and species, where frequency of occurrence was calculated as the number of samples in which the taxa (either phyla or species) was present, divided by the total number of sequenced samples of that sample type. Multivariate analyses were used to compare the detritus (suction and tray) from 2018 and 2019. A non-metric multidimensional scaling (NMDS) biplot based on the Jaccard similarity measure was used to visualize differences among detritus types. ESV identifications were converted to presence/absence values at the level of taxonomic order. Ellipses generated from the standard error of the weighted average of the scores in each treatment habitat were superimposed on each biplot to visualize the dispersion of each detritus type. A permutational analysis of variance (PERMANOVA) was conducted to test the multivariate response of taxonomic order presence/absence across the detritus types. When PERMANOVAs were significant ($p < 0.05$) a similarity percentage analysis (SIMPER) was used to evaluate the contribution of each taxonomic order to differences between detritus types. All statistical analyses were performed in R (R Core Team 2020).

Results

Stable isotope analyses

315 Detritus $\delta^{13}C$ values ranged from -19.5 ‰ (2019 EAM detritus) to -14.4 ‰ (2019 tray
316 detritus), and source $\delta^{13}C$ values ranged from -27.7 ‰ (2019 BCM tissue) to -10.7 ‰ (2019
317 *Halisarca caerulea* tissue; Table S3). Detritus $\delta^{15}N$ values ranged from 0.2 ‰ to 2.7 ‰ (both
318 from 2019 EAM detritus), and source $\delta^{15}N$ values ranged from -2.6 ‰ (2018 sediment traps) to
319 5.5 ‰ (2018 *Scopalina ruetzleri* tissue). In general, $\delta^{15}N$ values were greater in sponge tissue
320 samples than algae and BCM tissue samples (Fig. 1; Table S4). The isotope signatures of the
321 feces of spongivorous fishes (*Holacanthus ciliaris*, *Pomacanthus paru*) were similar to sponge
322 tissues, and the isotope signatures of the feces of herbivorous fishes (*Acanthurus bahianus*,
323 *Acanthurus coeruleus*) were similar to algae tissues (Fig. 1; Table S3–4).
324 There were notable seasonal changes in stable isotope compositions of some composite
325 and tissue samples between July 2018 and March 2019. For the $\delta^{15}N$ values of sediment trap
326 samples, there was a large increase and shift from negative to positive $\delta^{15}N$ values from 2018
327 (mean ± SD = -1.1 ± 1.3 ‰) to 2019 (-1.7 ± 0.5 ‰; Table S4). The emergent sponge species *A.*
328 *cauliformis* and cryptic sponge species *Chondrilla* sp. exhibited similar isotopic values, and both
329 exhibited increasing $\delta^{13}C$ values and decreasing $\delta^{15}N$ values from 2018 to 2019 (Fig. 1; Table
330 S3-4). The $\delta^{13}C$ of the cryptic sponge species *Halisarca caerulea* also increased from -17.9 ± 1.4
331 ‰ to -12.6 ± 2.8 ‰, and the $\delta^{13}C$ of BCM decreased markedly from -21.1 ± 0.1 ‰ to -27.1 ± 0.5
332 ‰, and this was the only tissue sample type with reduced $\delta^{13}C$ values in 2019 (Table S3).
333 The Bayesian isotope mixing model based on $\delta^{13}C$ and $\delta^{15}N$ values was used to establish
334 the relative contribution of each source to the detritus samples (Fig. 1). For 2018 samples, algae
335 and herbivore feces were pooled after initial runs indicated a high correlation between the sample
336 types (correlation = -0.72). The resulting model showed further correlations between the
337 combined algae/herbivore feces source category and BCM tissue and sediment trap samples

(correlation = -0.63, -0.74 respectively); these were further pooled into a category "algae/BCM/herbivore feces/sediment trap" (Fig. S1). The resulting model indicated high contribution by the pooled four source mixture to the EAM detritus (mean ± SD = 58.3 ± 11.1%), with the other source categories showing much lower contribution (< 8.5%; Fig. 2A). Earlier iterations of the model with unpooled sources showed high contribution by algal tissue and herbivore feces (44.8 ± 17%, 11.9 ± 14.5%, respectively; Fig. S2), suggesting the disproportionate contribution was not merely a byproduct of the pooling of four sources.

The mixing model of 2019 EAM detritus samples showed no major correlations among detrital sources, thus analyses proceeded on the original model with unpooled sources. The mixing model revealed similarly low contributions with large confidence intervals for all sources, ranging from 4.5 ± 3.3% for BCM tissue to 16 ±13.5% for algal tissue (Fig. 2B), and likely owing to the greater variability in EAM detritus isotopic values and tighter clustering of source samples around the EAM detritus (Fig. 1B). The tray detritus mixing model showed similarly low contributions and large confidence intervals for all sources (Fig. 2c).

Metabarcoding analyses

A total of 119,012,810 sequence reads were generated with a mean of 577,732 (± 302,189 SD) DNA sequence reads retained per sample per marker after bioinformatic filtering. The 18S marker yielded a mean of 1,121 (± 2,991 SD) ESVs per sample, COI yielded a mean of 452 (± 390 SD) ESVs per sample, and 16S yielded a mean of 11,657 (± 26,518 SD) ESVs per sample. Approximately 37.5% of ESVs (295,497 ESVs) were assigned taxonomy based on the selection criteria outlined in the methods.

Genetic sequences of tissue samples largely matched the morphology-based taxonomy (Table S5). Three out of four sponge species analyzed were identified to the genus level, and the

fourth sponge species (*Halisarca caerulea*) was identified at the family level (Halisarcidae), with the expected genus *Halisarca* scoring a 96%, just below the 98% threshold. The BCM was assigned the expected species *Moorea producens*, and *Lobophora* was assigned its proper genus. The tissue samples from the alga visually identified as *Dictyota* matched to multiple taxa, including phaeophyte genus *Dictyopteris* and rhodophytes in family rhodomelaceae including *Lomentaria* and *Neosiphonia*.

The composite samples (EAM and tray detritus, as well as source samples from sediment traps and the feces of herbivores and spongivores) contained rich genetic diversity. For the following analyses, we retained eukaryotes and cyanobacteria and excluded Archaea and bacteria other than cyanobacteria. A total of 17 metazoan phyla and 20 phyla from other kingdoms were identified in the composite samples (Fig. 3). Of these phyla, 34 were found in detritus (4 unique), 27 were found in sediment trap samples (0 unique), 23 were found in herbivore feces (0 unique) and 21 were found in spongivore feces (2 unique; Fig. 3). Metazoan phyla Arthropoda, Nematoda, Xenacoelomorpha, Annelida, Mollusca, and Porifera were found in over 50% of EAM detritus samples. The most frequent phylum, Arthropoda, was detected in 82% of EAM detritus samples, while Porifera was detected in 55% of EAM detritus samples. Metazoan phyla Arthropoda, Porifera, Chordata, Cnidaria, and Mollusca were found in over 50% of sediment trap samples, and the most frequent phyla were Porifera and Arthropoda (83% each). Metazoan phyla Chordata, Cnidaria, Porifera, and Platyhelminthes were found in over 50% of spongivore feces samples, and the most frequent phyla were Chordata and Cnidaria (80% each) while Porifera was detected in 60% of samples. No metazoan phyla were found in more than 50% of herbivore feces samples (Fig. 3).

On average, non-metazoan phyla had higher frequencies of occurrence than metazoan phyla (Fig. 3). Bacillariophyta, Rhodophyta, Cyanobacteria, and Ciliophora were detected in at least 90% of EAM detritus samples, and those four phyla as well as Chlorophyta, Cercozoa, and Haptista were detected in at least 90% of sediment trap samples. Bacillariophyta, Cyanobacteria and Rhodophyta were detected in at least 90% of herbivore feces samples, and Chlorophyta and Streptophyta were detected in 58% and 50% of herbivore feces samples, respectively. Streptophyta was detected in 100% of spongivore feces samples (Fig. 3).

The main taxa of interest in investigating the sponge-loop hypothesis were sponges, algae, and cyanobacteria. In total, we identified 36 sponge taxa spanning 14 families, 13 genera, and 6 species (Fig. 4). Multiple sponge taxa were detected in detritus, sediment trap, and spongivore feces samples, including all the sponge taxa identified from the tissue samples, except the family Halisarchidae. However, sponge taxa had very low frequencies of occurrence compared to other algae and metazoans (Fig. 4), and only two of the 36 taxa were detected in more than one of the 11 EAM detritus samples.

Among the algae (including Cyanobacteria), we identified 25 classes, 107 orders, 163 families, 202 genera, and 159 species. The most frequently detected taxa in detritus samples were also among the most frequently detected taxa in sediment trap samples as well as herbivore feces samples but were less frequent in spongivore feces samples (Fig. 4; Table S6). The cyanobacterium in the provided reference tissue sample was only detected in EAM and tray detritus, while the *Lobophora* algae identified from the tissue samples was detected in all sample types (Table S6). The *Dictyota* algae tissue did not yield consistent taxonomic identifications and the best algal matches from two samples (family Rhodomelaceae and genus *Dictyopteris*) were detected in EAM detritus, sediment trap samples, and herbivore feces (Table S6).

Metazoans other than Porifera also contributed to detritus. The most frequent metazoan taxa were harpacticoid copepods (phylum Arthropoda), identified in all the EAM detritus samples collected in July 2018 and half of the EAM detritus samples collected in March 2019. Cyclopoid copepods were also well represented in the EAM detritus collected in both years (Fig. 4). Among macrofaunal metazoans, the most frequently occurring in EAM included cnidarians of class Anthozoa (octocorals; Fig. 4), while cnidarians of class Scleractinia (hard corals) were notably scarce, with only one identification in a single EAM sample collected in 2018 (Table S7). Meiofaunal and epifaunal metazoans were more frequent than macrofauna, and Xenacoelomorpha (class Acoela), Platyhelminthes, and Nematoda were frequent in EAM detritus collected in both years (Fig. 4).

There were some notable differences among 2018 and 2019 EAM and tray detritus. The most immediate difference was the number of detected ESVs, and the number of detected ESVs in 2018 EAM detritus (7135 ± 8220 ESVs per sample) outnumbered tray detritus (4150 ± 4164 ESVs per sample) and greatly outnumbered 2019 EAM detritus (466 ± 435 ESVs per sample). There was also relatively low overlap of individual ESVs across seasons, only 245 of the total 34226 ESVs detected in EAM detritus were present in at least one sample from each season.

The NMDS based on presence-absence of taxonomic orders revealed separation of 2018 and 2019 EAM detritus (Fig. S3). Interestingly, tray detritus collected in 2019 was more similar to 2018 EAM detritus than 2019 EAM detritus, but this may be due to greater similarity in the number of detected ESVs in tray and 2018 EAM. PERMANOVA revealed significant differences in the communities (PERMANOVA $F_{2, 12} = 1.7636$, $p = 0.029$), and pairwise PERMANOVA indicated significant differences between the 2018 and 2019 EAM detritus

(adjusted p = 0.024). The phylum with the greatest contribution to dissimilarity was Bacillariophyta (SIMPER: 11.1%).

Frequency of occurrence data revealed some additional potential drivers of dissimilarity between the 2018 and 2019 EAM detritus samples. For the algae and cyanobacterial taxa, 41 of the top 50 most frequent algae taxa were present in 100% of 2018 EAM detritus samples, while only 3 of the top 50 taxa were present in 100% of 2019 EAM detritus samples (Table S6). Additionally, sequences matching to collected algae tissues were more frequent in 2018 EAM detritus compared to 2019 EAM detritus, particularly *Lobophora* (Table S6).

Discussion

The detritus in the epilithic algal matrix (EAM) on the Carrie Bow Cay forereef was derived from numerous benthic and pelagic sources. Primary producers were the dominant group of organisms contributing to detritus, consistent with previous studies (Hatcher 1983; Alongi 1988; Wilson et al. 2001, 2003). There was genetic signature of sponges (phylum Porifera) in detritus, but detritus contained low frequencies of Porifera sequences compared to primary producers and other metazoans, and detritus isotopic signatures were distinct from isotopic signatures of sponge tissues, indicating minimal sponge inputs to detritus. The use of complementary analyses and seasonal sampling herein yielded additional insights into how physical conditions (flow, currents, turbidity) may influence detritus composition.

Minimal sponge inputs to detritus

The results of this study are at odds with the detrital component of the sponge loop hypothesis, which proposed that "sponges transform a majority of DOM into particulate detritus" as shed sponge cells with "DOM turnover by sponges approaching the daily gross primary production of the entire reef ecosystem" (~~p. 110,~~ de Goeij et al 2013). Detritus contributions by

sponges were proposed to be approximately 6-fold greater than contributions from other sources (Fig. 3, de Goeij et al 2013). Considering these estimates and that the expected form of sponge-derived detrital material is cellular debris, the sponge signal from eDNA and stable isotopic signatures of forereef detritus samples should have been substantial, but it was not.

The six sponges sampled here are common species that represented a cross section of sponge diversity on Caribbean reefs (Loh and Pawlik 2014). This diversity was evident in the range of isotopic space that species occupied, and such isotopic differences can be attributed to species-specific diets, microbiomes, and nitrogen cycling and fractionation pathways (Freeman et al. 2021, van Duyl et al. 2018). Despite a diverse sampling of sponge species, isotope mixing models indicated low contribution by any species, consistent with the much lower frequencies of occurrence of Porifera sequences compared to algae and metazoans, especially when higher-order taxonomic groupings are compared. While frequencies are not true measurements of relative abundance of these diverse organisms, previous studies have demonstrated that DNA frequencies can approximate community abundance (Yoccoz et al. 2012), and low frequencies of Porifera sequences also paralleled differences between sponge and detritus isotopic signatures.

The deployment of trays under reef overhangs in 2019 was a generous test of the sponge loop hypothesis designed to maximize the odds of capturing choanocytes shed by cryptic sponge species. The three cryptic sponge species targeted in the present study (*Halisarca caerulea*, *Chondrilla caribensis*, and *Scopalina ruetzleri*) were also the same species for which detritus production has been measured and cited to support the sponge loop hypothesis, with *H. caerulea* being the most frequently used target species for these studies (de Goeij et al. 2008a, 2008b; De Goeij et al. 2009; de Goeij et al. 2013; Lesser et al. 2020; Campana et al. 2021; Hudspith et al. 2021). Notably, none of the EAM or tray detritus samples collected in the present study

474 contained sequences matching to *H. caerulea* (or *Halisarca*), despite the relative abundance of
475 this species on the Carrie Bow Cay forereef. Sequences matching to *S. ruetzleri* and *Chondrilla*
476 sp. were also absent from all detritus samples, except for one identification of *Chondrilla* sp. in
477 one of the two sequenced tray detritus samples. The absence of these species in the EAM, where
478 detritivore grazing occurs (Hatcher 1983), calls into question the ecological relevance of any
479 detritus they may produce.

480 *Detritus inputs by algae and non-sponge metazoans*

481 Isotope mixing models revealed a significant contribution of benthic macroalgae to EAM
482 detritus collected in 2018, and genetic analyses revealed a high frequency of sequences from
483 major plant phyla. These findings are congruent with reports that benthic and filamentous algae
484 are important contributors to coral reef detritus (Wilson et al. 2001). The benthic cover of
485 *Dictyota* experienced historical increases at Carrie Bow Cay likely due to removal of herbivores
486 by overfishing, but a ban on the harvest of herbivorous fishes in Belize has led to the recovery of
487 herbivore populations in recent years (Cox et al. 2013; Mumby and Steneck 2018; de Pablo et al.
488 2021). Not only do herbivore fish benefit the reef by minimizing algae cover, but their ceaseless
489 grazing and frequent defecations also act as a pathway to recycle algae tissue to the benthos as
490 detritus (Wernberg et al. 2006), and fish egestion of organic matter contain more nutrients than
491 their excretion of inorganic matter (Schiettekatte et al. 2023). A similar function is likely
492 performed by spongivore grazers. Indeed, the feces of prominent spongivore species
493 (*Holacanthus ciliaris* and *Pomacanthus paru*, Randall and Hartman 1968) matched isotopic
494 values of sponge tissues and contained Porifera sequences. However, spongivore feces were
495 isotopically and genetically distinct from EAM detritus, suggesting minimal detritus
496 contributions through the spongivore grazing pathway.

Pelagic sources were well represented in EAM detritus, consistent with the pelagic signature found in detritus collected from the forereef of Palmyra Atoll (Max et al. 2013). Every EAM detritus sample contained Bacillariales and Naviculales, orders of diatoms (phylum Bacillariophyceae) known for being among the most abundant microalgal components of detritus, accounting for up to 14% of detrital organic material, and likely contributing important dietary resources such as fatty acids and proteins (reviewed in Wilson et al. 2003). Many EAM detritus samples also contained crustacean signatures at lower overall frequencies, which may represent zooplankton or their feces that have arrived at the EAM through sinking or grazing by the "wall of mouths" (Hamner et al. 1988). Meiofaunal and epifaunal sequences were also abundant in the detritus, likely from living inhabitants of the EAM that are not part of the detritus but may consume it. Sequences matching to copepod order Harpacticoida were notably abundant in EAM detritus, consistent with past observations that harpacticoid copepod nauplii were the most numerically dominant members of the zooplankton on the Carrie Bow Cay forereef (Fornshell 1994). The xenacoelomorph order Acoela was also found in 73% of detritus samples, and a diversity of these meiofaunal flatworms are known to inhabit the shallow sediments of Carrie Bow Cay (Achatz et al. 2007; Hooge and Tyler 2008). Nematoda were also abundant, but are unlikely to interfere or compete with detritivore grazers (Leduc and Probert 2009).

The most common macrofaunal metazoans in EAM detritus were Mollusca (55% frequency) and Cnidaria (45% frequency). Identified molluscs included cephalaspidean gastropods in the family Haminoeidae, which may have been a non-selective detritivore grazer akin to other species in this family (Malaquias et al. 2004). Scleractinia (hard corals) were largely absent from EAM detritus. This was unexpected considering longstanding assertions about the importance of coral mucus to reef detritus (Gottfried and Roman 1983), but missing

identifications may also be due to the lack of cellular material containing the targeted genetic sequences in coral mucus. Interestingly, most cnidarian identifications in detritus belonged to octocorals (Order Alcyonacea). Gorgonian octocorals are abundant on Carrie Bow Cay but have received relatively less research attention (Kupfner Johnson and Hallock 2020). No reports or studies could be found addressing detrital contributions by octocorals, but further study is merited considering the findings herein of abundance of octocoral sequences in detritus.

Unusually negative $\delta^{15}N$ in water column particulates collected in sediment traps

The purpose of sediment traps was to capture the particulates sinking from the water column and distinguish them from particulates originating on the benthos. Lower $\delta^{13}C$ values of sediment trap particulates compared to benthic detritus were consistent with previous findings (Max et al. 2013) and in agreement with the pattern of generally lower $\delta^{13}C$ in phytoplankton compared to benthic autotrophs (van Duyl et al. 2018). Samples from the Palmyra atoll forereef exhibited comparable $\delta^{15}N$ values between sediment trap and EAM detritus, indicating a similar pelagic origin and highlighting the importance of pelagic inputs to forereef detritus (Max et al. 2013). In contrast, the isotopic signatures of Carrie Bow Cay forereef detritus suggest a combination of pelagic and benthic inputs, as $\delta^{15}N$ of sediment trap particulates was highly reduced compared to EAM detritus, even taking on an unusually negative value in 2018. The observation of lower $\delta^{15}N$ in sediment traps (pelagic particulates) compared to EAM detritus (benthic particulates) contradicts other reports of elevated $\delta^{15}N$ in pelagic compared to benthic organic matter (van Duyl et al. 2018). This trend reversal may be due to unique circumstances driving negative $\delta^{15}N$ in waters around Carrie Bow Cay and reflected in the sediment trap samples in 2018, and two possible explanations for negative $\delta^{15}N$ are presented below.

First, uncharacteristically negative $\delta^{15}N$ values for detritus in sediment traps from July 2018 samples may be a result of grazing by zooplankton on the diazotrophic cyanobacterium *Trichodesmium.* Similarly negative $\delta^{15}N$ values (-1 to -2 ‰) of zooplankton collected from oligotrophic waters were attributed to nitrogen fixation by *Trichodesmium* that are consumed by zooplankton (Montoya et al. 2002). *Trichodesmium* is abundant during the summer at Carrie Bow Cay, and the forereef may act as a sink of *Trichodesmium* (Villareal 1995). We identified *Trichodesmium* in two EAM detritus samples from 2018 (40% frequency of occurrence) and zero sediment trap samples; *Trichodesmium* colonies were likely either retained in the 150 μm prefilter or grazed, for example by cyanobacteria-grazing mixotrophic dinoflagellates such as *Alexandrium* (Jeong et al. 2010). *Alexandrium* was found in 80% of 2018 sediment traps but missing from all other composite samples. This dinoflagellate could have contributed to uniquely negative $\delta^{15}N$ values of organic matter if it arrived in large quantities after grazing on *Trichodesmium*. We were unable to measure the relative abundance of *Alexandrium,* but this explanation is consistent with reports of sharply declining abundances of *Trichodesmium* across the Carrie Bow Cay forereef for which zooplankton grazing was implicated as a likely cause (Villareal 1995).

A second explanation could be that nitrogen in the atmosphere and rain is notably depleted in ^{15}N around Carrie Bow Cay, and the $\delta^{15}N$ values of nearby nutrient-starved mangroves can be as low as -17 (Fogel et al. 2008). Currents may carry particulates from the ^{15}N-depleted mangroves from the lagoon, through the tidal cut, and onto the reef. However, July is marked by northeasterly trade winds and a net onshore current flow (Greer and Kjerfve 1982; Koltes and Opishinski 2009) that flushes the forereef with more oceanic than lagoonal seawater. Irrespective of the origin of ^{15}N-depleted particles in sediment traps, whether open ocean or

lagoon, the isotopic and genetic distinctions between sediment trap particulates and EAM detritus indicate separate origins and composition of the particulates in July 2018.

Seasonal differences in sources and composition of detritus

There were considerable seasonable shifts in the isotopic signatures of several detritus sources between July 2018 and March 2019. Tissue samples of the HMA sponge species *Aplysina cauliformis* and *Chondrilla* sp. exhibited a rise in $\delta^{13}C$, perhaps because higher irradiance and water clarity led to more CO_2 fixation by the sponge photosymbionts and consequently lower $\delta^{13}C$ of these sponge species in July 2018, compared to March 2019 when reduced irradiance may have favored heterotrophy. The $\delta^{13}C$ shifts in tissues of other sponge species reflected their different feeding strategies and dietary preferences. The overlap in $\delta^{13}C$ between EAM detritus and the tissues of *Niphates digitali*s is consistent with the detritus-dominated diet of this species (Freeman et al. 2021). The DOC-dominated diets of *X. muta* and *H. caerulea* (de Goeij et al. 2008a; McMurray et al. 2018) may also explain the seasonal rise in $\delta^{13}C$ values in their tissues, for example if there was a shift from pelagic to benthic sources of DOC; *X. muta* consumes DOC of varying pelagic and benthic origins, depending on environmental availability (van Duyl et al. 2018).

There was a collective decline in the $\delta^{15}N$ values of tissues of all six sponge species in March 2019, suggesting widespread changes to nitrogen taken up by sponges from their environment. The sponge microbiome can also influence $\delta^{15}N$ in complex ways (van Duyl et al. 2018) and may explain why some species showed larger $\delta^{15}N$ reductions than others. For example, the connection between nitrogen fixation and reduced $\delta^{15}N$ (Southwell et al. 2008) may explain larger $\delta^{15}N$ reductions in *A. cauliformis*, which relies on symbionts for nutrition,

compared to the smaller $\delta^{15}N$ reductions in *N. digitalis*, which predominantly depends on external nitrogen sources (Weisz et al. 2007).

Samples of tissues from benthic cyanobacterial mats (BCM) exhibited an unexpected drop in $\delta^{13}C$ values. This is the first known report of such a seasonal shift for BCM, and it may be due to seasonal variation in dissolved inorganic carbon (DIC) or BCM species composition. Sequencing was only performed on BCM samples from July 2018, precluding seasonal comparison of the species known to occur in the BCM consortia (e.g., *Moorea, Oscillatoria, Hydrocoleum*).

Although isotopic and genetic signatures of detritus sources varied from July 2018 to March 2019, isotopic signatures of the detritus itself remained relatively consistent between the seasons. EAM detritus contained an abundance of sequences matching to primary producers whose mechanical breakdown and predation can directly contribute to detritus (Wilson et al. 2003). The abundant dissolved organic matter (DOM) produced by benthic algae and other autotrophs may also spontaneously form polymer gels or adsorb to carbonate sediments and become a form of amorphic detritus (Otsuki and Wetzel 1973; Chin et al. 1998; Wilson et al. 2003). Amorphic detritus is a non-cellular composite undetectable by genetic sequencing methods but with an isotopic signature reflective of its source organism, and significant inputs of this form of detritus may explain similar isotopic signatures despite distinct genetic sequences in detritus from both seasons. Amorphic detritus is a form of molecularly uncharacterized materials, byproducts of complex biogeochemical processes that escape characterization by traditional chromatography-based techniques and are poorly understood across all aquatic ecosystems, especially coral reefs (Bowen 1979; Wilson 2002; Wilson et al. 2003; Wakeham and Lee 2019).

609 Multiple lines of evidence indicate that detritus composition was shaped by
610 environmental conditions on the forereef, namely higher flow and greater turbulence in March
611 2019 compared to July 2018. First, detritus collected in March 2019 had more variable isotopic
612 delta values and fewer genetic sequences compared to detritus collected in July 2018, indicating
613 a more heterogenous and scarce mixture that may result from greater turbulence and mixing.
614 Detritus collected in March 2019 was also characterized by greater frequency of meiofauna and
615 epifauna that likely inhabit the EAM, including Annelida, Nematoda, and Xenacoelomorpha, and
616 lower frequencies of macrofauna that originated elsewhere on the benthos, pointing to surge-
617 driven export of macrofaunal-derived organic matter before it could settle and get trapped in the
618 EAM in March 2019. Stronger surge conditions may have also caused the resuspension of
619 benthic particulates in the water column, which would account for the presence of sequences
620 belonging to benthic metazoans (e.g., Porifera, Mollusca, Cnidaria) in sediment trap samples in
621 March 2019. Sediment traps are effective water column samplers when conditions are calm (flow
622 < 0.2 m/s), as was the case during July 2018 sampling, but sediment traps may capture
623 resuspended benthic materials when conditions are turbulent as was the case during March 2019
624 sampling (Gardner 1980; White 1990; Wilson et al. 2003). The more energetic environment in
625 March 2019 may have also amplified production of amorphic detritus in the EAM, as DOM
626 aggregation may be facilitated by more encounters with substrates and increased laminar shear
627 and bubbles formed in the higher water motion (Wilson et al. 2003).
628 *Ecological implications*
629 Organic matter cycling through the detrital food web is complicated by the number of
630 organisms that may act as both sources and sinks of detritus, including bacteria, sponges,
631 surgeonfishes, and parrotfishes (Choat et al. 2002; Wilson et al. 2003; Crossman et al. 2005;

632 Dromard et al. 2015; Mumby and Steneck 2018). It is important to understand how detritus is
633 processed and transformed by these groups. Certain detritivores can selectively reduce protein
634 levels on the reef, resulting in higher carbon-to-nitrogen ratios and decreased nutritional value in
635 nitrogen-limited systems, as observed in the backreef habitats of Palmyra Atoll in the Pacific
636 Ocean (Max et al. 2013). Detritus is likely more abundant on Caribbean coral reefs (Mumby and
637 Steneck 2018), and there may be a surplus of nutritious detritus on the Carrie Bow Cay forereef
638 due to the windward exposure of the reef and other favorable conditions driving import of
639 particulate matter onto the reef.

640 The higher productivity in the Summer (July 2018) and potential influx of sinking phyto-
641 and zooplankton may have supplemented benthic sources of detritus, while the more energetic
642 early spring (March 2019) resulted in greater mixing and flushing and perhaps better conditions
643 for formation and accumulation of amorphic detritus in the EAM. Seasonal conditions may bring
644 a variety and surplus of detritus that is regularly replenished to the forereef and may even supply
645 downstream backreef and lagoonal habitats (Hatcher 1983). Despite an abundance of detritus,
646 there may be an imbalance in the number of detritivores feeding on it, as detritivores are less
647 diverse and abundant in the Caribbean compared to Pacific reefs (Bellwood et al. 2004; Roff and
648 Mumby 2012; Edwards et al. 2014). A shortage of detritivores in the Caribbean may leave this
649 overflow detritus to get recycled into the microbial loop, returned to benthic suspension feeders
650 (e.g., sponges), or lost from the reef system (Mumby and Steneck 2018).

651 The breadth of sampling conducted in the present study (16 tissue and composite sample
652 types collected over 2 seasons) encompassed many common organisms and the most likely
653 candidates for detritus production, although this sample breadth limited the number of replicates
654 from each group that could feasibly be analyzed. The stable isotope analyses and eDNA

metabarcoding analysis methods used herein each had limitations that the other method accounted for to some degree, but some gaps remained. Isotope mixing models can only estimate contributions of sampled sources, so while this was an expansive sampling effort, it was not exhaustive, and detritus isotopic signatures may have been influenced by diagenetic changes, especially of $\delta^{15}N$ values (Caraco et al. 1998). Genetic sequencing complemented the isotopic analyses by identifying all traces of organisms that are cataloged and with genetic material that resisted degradation, but some organisms could have escaped detection if they were novel or degraded (Reef et al. 2017). The omission of bacteria besides cyanobacteria in the genetic sequence data also discounted a key component of detritus (Biddanda 1985; Alongi 1988; Wilson et al. 2003), but the bacterial signal would have been present in the isotopic signatures of detritus.

To better understand how reefs of the future will function, it is crucial to understand how energy is transferred throughout contemporary coral reefs, including the complex and poorly-elucidated detrital pathway. While sponges may not be major contributors through direct production of detritus, they may extend the residence time of organic matter on coral reefs through efficient uptake of DOC and accumulation of biomass that is eventually grazed or mechanically broken down and returned to the detrital pool. This carbon pathway may not be essential to the healthy functioning of Caribbean coral reefs, however, considering low demand by relatively few detritivorous grazers. As benthic communities continue to shift from coral- to algae- or sponge- dominated systems, this will alter trophodynamics and influence the detrital resources on which these systems rely.

Acknowledgements

Many thanks to Laura Gaitan Daza, Steve McMurray, Jim Evans, Mellissa Dionesotes, and Sasha Giametti for assistance in the field, the staff of Smithsonian Institution's Carrie Bow Cay Field Station in Belize for logistical support, Evan Heit and Kim Rosov for assistance with preparation and analyses of stable isotope samples, and Nicole Fogarty and Amy Grogan for additional assistance with reviewing and providing input on earlier drafts of this manuscript. This is contribution #### from Carrie Bow Cay field station.

References

Achatz JG, Hooge MD, Tyler S (2007) Convolutidae (Acoela) from Belize. Zootaxa 1479:35–66

Alongi DM (1988) Detritus in coral reef ecosystems: fluxes and fates. Proc 6th Int Coral Reef Symp 1:29-36

Altschul SF, Gish W, Miller W, Myers EW, Lipman DJ (1990) Basic local alignment search tool. J Mol Biol 215:403–410

Aronson RB, Precht WF, Toscano MA, Koltes KH (2002) The 1998 bleaching event and its aftermath on a coral reef in Belize. Mar Biol 141:435–447

Azam F, Fenchel T, Field J, Gray J, Meyer-Reil L, Thingstad F (1983) The ecological role of water-column microbes in the sea. Mar Ecol Prog Ser 10:257–263

Baird DJ, Hajibabaei M (2012) Biomonitoring 2.0: a new paradigm in ecosystem assessment made possible by next-generation DNA sequencing. Mol Ecol 21:2039–2044

de Bakker DM, van Duyl FC, Bak RPM, Nugues MM, Nieuwland G, Meesters EH (2017) 40 Years of benthic community change on the Caribbean reefs of Curaçao and Bonaire: the rise of slimy cyanobacterial mats. Coral Reefs 36:355–367

700 Begon M, Harper JL, Townsend CR (1986) Ecology: individuals, populations and communities.
701 Blackwell scientific publications
702 Bellwood DR, Hughes TP, Folke C, Nyström M (2004) Confronting the coral reef crisis. Nature
703 429:827–833
704 Biddanda B (1985) Microbial synthesis of macroparticulate matter. Mar Ecol Prog Ser 20:241–
705 251
706 Bowen SH (1979) A nutritional constraint in detritivory by fishes: The stunted population of
707 *Sarotherodon mossambicus* in Lake Sibaya, South Africa. Ecol Monogr 49:17–31
708 Boyi JO, Heße E, Rohner S, Säurich J, Siebert U, Gilles A, Lehnert K (2022) Deciphering
709 Eurasian otter (*Lutra lutra* L.) and seal (*Phoca vitulina* L.; *Halichoerus grypus* F.) diet:
710 metabarcoding tailored for fresh and saltwater fish species. Molecular Ecology 31:5089–
711 5106
712 Brocke HJ, Piltz B, Herz N, Abed RMM, Palinska KA, John U, den Haan J, de Beer D, Nugues
713 MM (2018) Nitrogen fixation and diversity of benthic cyanobacterial mats on coral reefs
714 in Curacao. Coral Reefs 37:861–874
715 Brocke HJ, Wenzhoefer F, de Beer D, Mueller B, van Duyl FC, Nugues MM (2015) High
716 dissolved organic carbon release by benthic cyanobacterial mats in a Caribbean reef
717 ecosystem. Sci Rep 5:8852
718 Callahan BJ, McMurdie PJ, Rosen MJ, Han AW, Johnson AJA, Holmes SP (2016) DADA2:
719 High-resolution sample inference from Illumina amplicon data. Nat Methods 13:581–583
720 Campana S, Hudspith M, Lankes D, de Kluijver A, Demey C, Schoorl J, Absalah S, van der
721 Meer MTJ, Mueller B, de Goeij JM (2021) Processing of naturally sourced macroalgal-

722 and coral-dissolved organic matter (DOM) by high and low microbial abundance
723 encrusting sponges. Front Mar Sci 8:640583
724 Caraco N, Lampman G, Cole J, Limburg K, Pace M, Fischer D (1998) Microbial assimilation of
725 DIN in a nitrogen rich estuary: Implications for food quality and isotope studies. Mar
726 Ecol Prog Ser 167:59–71
727 Chin W-C, Orellana MV, Verdugo P (1998) Spontaneous assembly of marine dissolved organic
728 matter into polymer gels. Nature 391:568–572
729 Choat J, Clements K, Robbins W (2002) The trophic status of herbivorous fishes on coral reefs.
730 Mar Biol 140:613–623
731 Cox CE, Jones CD, Wares JP, Castillo KD, McField MD, Bruno JF (2013) Genetic testing
732 reveals some mislabeling but general compliance with a ban on herbivorous fish
733 harvesting in Belize: genetic testing on coral reef fish in Belize. Conserv Lett 6:132–140
734 Crossman D, Choat J, Clements K (2005) Nutritional ecology of nominally herbivorous fish on
735 coral reefs. Mar Ecol Prog Ser 296:129–142
736 Crossman DJ, Choat HJ, Clements KD, Hardy T, McConochie J (2001) Detritus as food for
737 grazing fishes on coral reefs. Limnol Oceanogr 46:1596–1605
738 Darwin C, Bonney TG (1896) The structure and distribution of coral reefs. D. Appleton and
739 Company, New York
740 Done TJ (1992) Phase shifts in coral reef communities and their ecological significance.
741 Hydrobiologia 247:121–132
742 Dromard CR, Bouchon-Navaro Y, Harmelin-Vivien M, Bouchon C (2015) Diversity of trophic
743 niches among herbivorous fishes on a Caribbean reef (Guadeloupe, Lesser Antilles),
744 evidenced by stable isotope and gut content analyses. J Sea Res 95:124–131

745 van Duyl FC, Moodley L, Nieuwland G, van Ijzerloo L, van Soest RWM, Houtekamer M,
746 Meesters EH, Middelburg JJ (2011) Coral cavity sponges depend on reef-derived food
747 resources: Stable isotope and fatty acid constraints. Mar Biol 158:1653–1666
748 van Duyl FC, Mueller B, Meesters EH (2018) Spatio–temporal variation in stable isotope
749 signatures ($\delta^{13}C$ and $\delta^{15}N$) of sponges on the Saba Bank. PeerJ 6:e5460
750 Edwards CB, Friedlander AM, Green AG, Hardt MJ, Sala E, Sweatman HP, Williams ID,
751 Zgliczynski B, Sandin SA, Smith JE (2014) Global assessment of the status of coral reef
752 herbivorous fishes: Evidence for fishing effects. Proc R Soc B Biol Sci 281:20131835
753 Fabricius KE (2005) Effects of terrestrial runoff on the ecology of corals and coral reefs: review
754 and synthesis. Mar Poll Bull 50:125–146
755 Fenchel T (2008) The microbial loop – 25 years later. J Exp Mar Biol Ecol 366:99–103
756 Fogel ML, Wooller MJ, Cheeseman J, Smallwood BJ, Roberts Q, Romero I, Meyers MJ (2008)
757 Unusually negative nitrogen isotopic compositions ($\delta^{15}N$) of mangroves and lichens in an
758 oligotrophic, microbially-influenced ecosystem. Biogeosciences 5:1693–1704
759 Fornshell JA (1994) Copepod nauplii from the barrier reef of Belize. Hydrobiologia 292:295–
760 301
761 Freeman CJ, Easson CG, Baker DM (2014) Metabolic diversity and niche structure in sponges
762 from the Miskito Cays, Honduras. PeerJ 2:e695
763 Freeman CJ, Easson CG, Fiore CL, Thacker RW (2021) Sponge–microbe interactions on coral
764 reefs: multiple evolutionary solutions to a complex environment. Front Mar Sci 8:705053
765 Gardner W (1980) Sediment trap dynamics and calibration: a laboratory evaluation. J Mar Res
766 38:17–39

767 de Goeij JM, van den Berg H, van Oostveen M, Epping E, van Duyl F (2008a) Major bulk
768 dissolved organic carbon (DOC) removal by encrusting coral reef cavity sponges. Mar
769 Ecol Prog Ser 357:139–151
770 de Goeij JM, Moodley L, Houtekamer M, Carballeira NM, van Duyl FC (2008b) Tracing ^{13}C-
771 enriched dissolved and particulate organic carbon in the bacteria-containing coral reef
772 sponge *Halisarca caerulea*: Evidence for DOM-feeding. Limnol Oceanogr 53:1376–
773 1386
774 de Goeij JM, de Kluijver A, van Duyl FC, Vacelet J, Wijffels RH, de Goeij AFPM, Cleutjens
775 JPM, Schutte B (2009) Cell kinetics of the marine sponge *Halisarca caerulea* reveal
776 rapid cell turnover and shedding. J Exp Biol 212:3892–3900
777 de Goeij JM, van Oevelen D, Vermeij MJA, Osinga R, Middelburg JJ, de Goeij AFPM,
778 Admiraal W (2013) Surviving in a marine desert: The sponge loop retains resources
779 within coral reefs. Science 342:108–110
780 Gottfried M, Roman MR (1983) Ingestion and incorporation of coral-mucus detritus by reef
781 zooplankton. Mar Biol 72:211–218
782 Greenwood NDW, Sweeting CJ, Polunin NVC (2010) Elucidating the trophodynamics of four
783 coral reef fishes of the Solomon Islands using δ^{15}N and δ^{13}C. Coral Reefs 29:785–792
784 Greer JE, Kjerfve B (1982) Water currents adjacent to Carrie Bow Cay, Belize. Smithson
785 Contrib Mar Sci 12:53–58
786 Hamner WM, Jones MS, Carleton JH, Hauri IR, Williams DM (1988) Zooplankton,
787 planktivorous fish, and water currents on a windward reef face: Great Barrier Reef,
788 Australia. Bull Mar Sci 42:21

789 Hatcher BG (1983) Role of detritus in the metabolism and secondary production of coral reef
790 ecosystems. Proc GBR Conf 317–25
791 Hoegh-Guldberg O, Mumby PJ, Hooten AJ, Steneck RS, Greenfield P, Gomez E, Harvell CD,
792 Sale PF, Edwards AJ, Caldeira K, Knowlton N, Eakin CM, Iglesias-Prieto R, Muthiga N,
793 Bradbury RH, Dubi A, Hatziolos ME (2007) Coral reefs under rapid climate change and
794 ocean acidification. Science 318:1737–1742
795 Hooge MD, Tyler S (2008) Acoela (Acoelomorpha) from Bocas del Toro, Panama. Zootaxa
796 1719:1–40
797 Hudspith M, Rix L, Achlatis M, Bougoure J, Guagliardo P, Clode PL, Webster NS, Muyzer G,
798 Pernice M, de Goeij JM (2021) Subcellular view of host–microbiome nutrient exchange
799 in sponges: insights into the ecological success of an early metazoan–microbe symbiosis.
800 Microbiome 9:44
801 Hughes TP (1994) Catastrophes, phase shifts, and large-scale degradation of a Caribbean coral
802 reef. Science 265:1547–1551
803 Jeong HJ, Yoo YD, Kim JS, Seong KA, Kang NS, Kim TH (2010) Growth, feeding and
804 ecological roles of the mixotrophic and heterotrophic dinoflagellates in marine planktonic
805 food webs. Ocean Sci J 45:65–91
806 Johnson C, Klumpp D, Field J, Bradbury R (1995) Carbon flux on coral reefs: Effects of large
807 shifts in community structure. Mar Ecol Prog Ser 126:123–143
808 Koltes KH, Opishinski TB (2009) Patterns of water quality and movement in the vicinity of
809 Carrie Bow Cay, Belize. Smithson Contrib Mar Sci 38:379–390

Kornder NA, Esser Y, Stoupin D, Leys SP, Mueller B, Vermeij MJA, Huisman J, Goeij JM de (2022) Sponges sneeze mucus to shed particulate waste from their seawater inlet pores. Curr Biol 32:3855–3861

Kramer MJ, Bellwood DR, Bellwood O (2012) Cryptofauna of the epilithic algal matrix on an inshore coral reef, Great Barrier Reef. Coral Reefs 31:1007–1015

Kupfner Johnson S, Hallock P (2020) A review of symbiotic gorgonian research in the western Atlantic and Caribbean with recommendations for future work. Coral Reefs 39:239–258

Leduc D, Probert PK (2009) The effect of bacterivorous nematodes on detritus incorporation by macrofaunal detritivores: a study using stable isotope and fatty acid analyses. J Exp Mar Biol Ecol 371:130–139

Lesser MP, Mueller B, Pankey MS, Macartney KJ, Slattery M, de Goeij JM (2020) Depth-dependent detritus production in the sponge, *Halisarca caerulea*. Limnology and Oceanography 65:1200–1216

Levinton, J. 2021 Marine Biology. 6th edition Oxford Univ. Press

Loh T-L, Pawlik JR (2014) Chemical defenses and resource trade-offs structure sponge communities on Caribbean coral reefs. Proc Natl Acad Sci USA 111:4151–4156

Malaquias MAE, Condinho S, Cervera JL, Sprung M (2004) Diet and feeding biology of *Haminoea orbygniana* (Mollusca: Gastropoda: Cephalaspidea). J Mar Biol Assoc U K 84:767–772

Martin M (2011) Cutadapt removes adapter sequences from high-throughput sequencing reads. EMBnet.journal 17:10–12

831 Max L, Hamilton S, Gaines S, Warner R (2013) Benthic processes and overlying fish
832 assemblages drive the composition of benthic detritus on a central Pacific coral reef. Mar
833 Ecol Prog Ser 482:181–195
834 McClenaghan B, Fahner N, Cote D, Chawarski J, McCarthy A, Rajabi H, Singer G, Hajibabaei
835 M (2020) Harnessing the power of eDNA metabarcoding for the detection of deep-sea
836 fishes. PLOS ONE 15:e0236540
837 McMurray SE, Stubler AD, Erwin PM, Finelli CM, Pawlik JR (2018) A test of the sponge-loop
838 hypothesis for emergent Caribbean reef sponges. Mar Ecol Prog Ser 588:1–14
839 Michener RH, Kaufman L (2007) Stable isotope ratios as tracers in marine food webs: an update.
840 In: Michener RH, Lajtha K (eds) Stable isotopes in ecology and environmental science.
841 John Wiley & Sons, Ltd, pp 238–282
842 Middelburg JJ (2014) Stable isotopes dissect aquatic food webs from the top to the bottom.
843 Biogeosciences 11:2357–2371
844 Montoya JP, Carpenter EJ, Capone DG (2002) Nitrogen fixation and nitrogen isotope
845 abundances in zooplankton of the oligotrophic North Atlantic. Limnol Oceanogr
846 47:1617–1628
847 Mumby PJ, Steneck RS (2018) Paradigm lost: dynamic nutrients and missing detritus on coral
848 reefs. BioScience 68:487–495
849 Norström AV, Nyström M, Lokrantz J, Folke C (2009) Alternative states on coral reefs: beyond
850 coral-macroalgal phase shifts. Mar Ecol Prog Ser 376:293–306
851 Otsuki A, Wetzel RG (1973) Interaction of yellow organic acids with calcium carbonate in
852 freshwater. Limnol Oceanogr 18:490–493

853 de Pablo LX, Lefcheck JS, Harper L, Paul VJ, Jones S, Whippo R, Seemann J, Kline DI, Duffy
854 JE (2021) A doubling of stony coral cover on shallow forereefs at Carrie Bow Cay,
855 Belize from 2014 to 2019. Sci Rep 11:19185
856 Parnell A (2019) simmr: a stable isotope mixing model. R package version 0.5.0.9000
857 Post DM (2002) Using stable isotopes to estimate trophic position: Models, methods, and
858 assumptions. Ecology 83:703–718
859 Purcell S, Bellwood D (2001) Spatial patterns of epilithic algal and detrital resources on a
860 windward coral reef. Coral Reefs 20:117–125
861 R Core Team (2020) R: a language and environment for statistical computing.
862 Randall JE, Hartman WD (1968) Sponge-feeding fishes of the West Indies. Mar Biol 1:216–225
863 Reef R, Atwood TB, Samper-Villarreal J, Adame MF, Sampayo EM, Lovelock CE (2017) Using
864 eDNA to determine the source of organic carbon in seagrass meadows. Limnol Oceanogr
865 62:1254–1265
866 Roff G, Mumby PJ (2012) Global disparity in the resilience of coral reefs. Trends Ecol Evol
867 27:404–413
868 Rützler K, Macintyre IG (1982) The habitat distribution and community structure of the barrier
869 reef complex at Carrie Bow Cay, Belize. Smithson Contrib Mar Sci 12:9–45
870 Schidlowski M (2001) Carbon isotopes as biogeochemical recorders of life over 3.8 Ga of Earth
871 history: evolution of a concept. Precambrian Res 106:117–134
872 Schiettekatte NMD, Casey JM, Brandl SJ, Mercière A, Degregori S, Burkepile D, Van Wert JC,
873 Ghilardi M, Villéger S, Parravicini V The role of fish feces for nutrient cycling on coral
874 reefs. Oikos n/a:e09914

875 Southwell MW, Weisz JB, Martens CS, Lindquist N (2008) In situ fluxes of dissolved inorganic
876 nitrogen from the sponge community on Conch Reef, Key Largo, Florida. Limnol
877 Oceanogr 53:986–996
878 Taberlet P, Coissac E, Hajibabaei M, Rieseberg LH (2012) Environmental DNA. Mol Ecol
879 21:1789–1793
880 Tebbett SB, Bellwood DR (2019) Algal turf sediments on coral reefs: What's known and what's
881 next. Mar Poll Bull 149:110542
882 Thomsen PF, Willerslev E (2015) Environmental DNA – An emerging tool in conservation for
883 monitoring past and present biodiversity. Biol Conserv 183:4–18
884 Villareal TA (1995) Abundance and photosynthetic characteristics of *Trichodesmium* spp. along
885 the Atlantic Barrier Reef at Carrie Bow Cay, Belize. Mar Ecol 16:259–271
886 Wakeham SG, Lee C (2019) Limits of our knowledge, part 2: Selected frontiers in marine
887 organic biogeochemistry. Mar Chemistry 212:16–46
888 Weisz JB, Hentschel U, Lindquist N, Martens CS (2007) Linking abundance and diversity of
889 sponge-associated microbial communities to metabolic differences in host sponges. Mar
890 Biol 152:475–483
891 Wernberg T, Vanderklift MA, How J, Lavery PS (2006) Export of detached macroalgae from
892 reefs to adjacent seagrass beds. Oecologia 147:692–701
893 White J (1990) The use of sediment traps in high-energy environments. Mar Geophys Res
894 12:145–152
895 Wilson S (2002) Nutritional value of detritus and algae in blenny territories on the Great Barrier
896 Reef. J Exp Mar Biol Ecol 271:155–169

Wilson S, Bellwood D, Choat J, Furnas M (2003) Detritus in the epilithic algal matrix and its use by coral reef fishes. Oceanogr Mar Biol: Annu Rev 41:279–309

Wilson S, Burns K, Codi S (2001) Identifying sources of organic matter in sediments from a detritivorous coral reef fish territory. Org Geochem 32:1257–1269

Wilson SK (2000) Trophic status and feeding selectivity of blennies (Blenniidae: Salariini). Mar Biol 136:431–437

Yoccoz NG, Bråthen KA, Gielly L, Haile J, Edwards ME, Goslar T, Von Stedingk H, Brysting AK, Coissac E, Pompanon F, Sønstebø JH, Miquel C, Valentini A, De Bello F, Chave J, Thuiller W, Wincker P, Cruaud C, Gavory F, Rasmussen M, Gilbert MTP, Orlando L, Brochmann C, Willerslev E, Taberlet P (2012) DNA from soil mirrors plant taxonomic and growth form diversity. Mol Ecol 21:3647–3655

Zapata-Hernández G, Sellanes J, Letourneur Y, Harrod C, Morales NA, Plaza P, Meerhoff E, Yannicelli B, Carrasco SA, Hinojosa I, Gaymer CF (2021) Tracing trophic pathways through the marine ecosystem of Rapa Nui (Easter Island). Aquat Conserv: Mar Freshw Ecosyst 31:304–323

912

Figure 1

Isotope biplots of samples collected in a) July 2018 and b) March 2019.

Detritus samples, including EAM and tray detritus, are represented by open and filled circles, respectively, that denote the values of individual samples. All other symbols represent the average ± SD of source samples

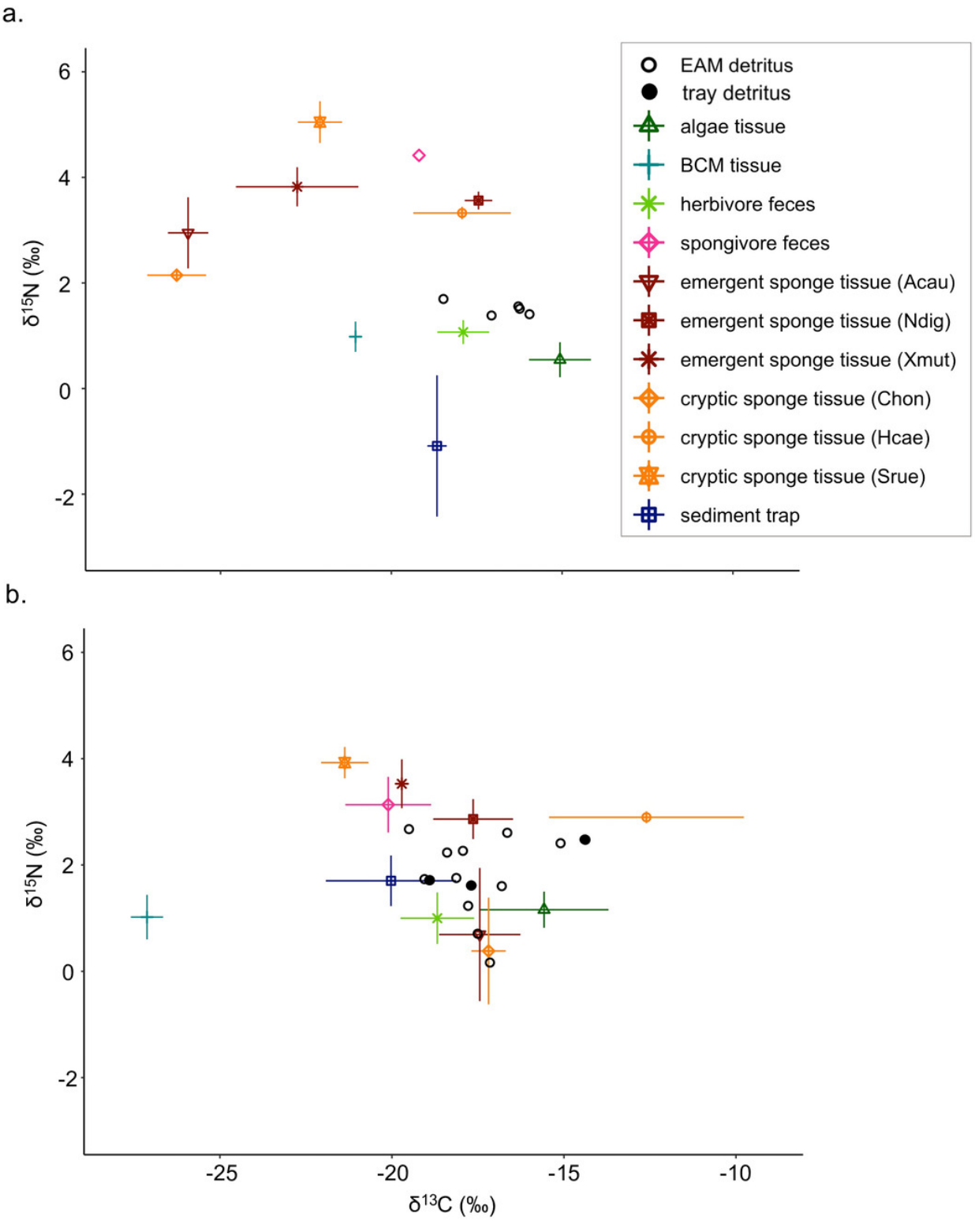
a.
6
4
2
0
-2
δ15N (‰)
EAM detritus
tray detritus
algae tissue
BCM tissue
herbivore feces
spongivore feces
emergent sponge tissue (Acau)
emergent sponge tissue (Ndig)
emergent sponge tissue (Xmut)
cryptic sponge tissue (Chon)
cryptic sponge tissue (Hcae)
cryptic sponge tissue (Srue)
sediment trap
b.
6
4
2
0
-2
δ15N (‰)
-25
-20
-15
-10
δ13C (‰)

Figure 2

Simulated contributions of each source to EAM detritus in a) July 2018 and b) March 2019, and to c) tray detritus in March 2019.

In the box plots, the boundary of the box closest to zero indicates the 25th percentile, a black line within the box marks the median, and the boundary of the box farthest from zero indicates the 75th percentile. Whiskers above and below the box indicate the 10th and 90th percentiles, and outermost points indicate outliers.

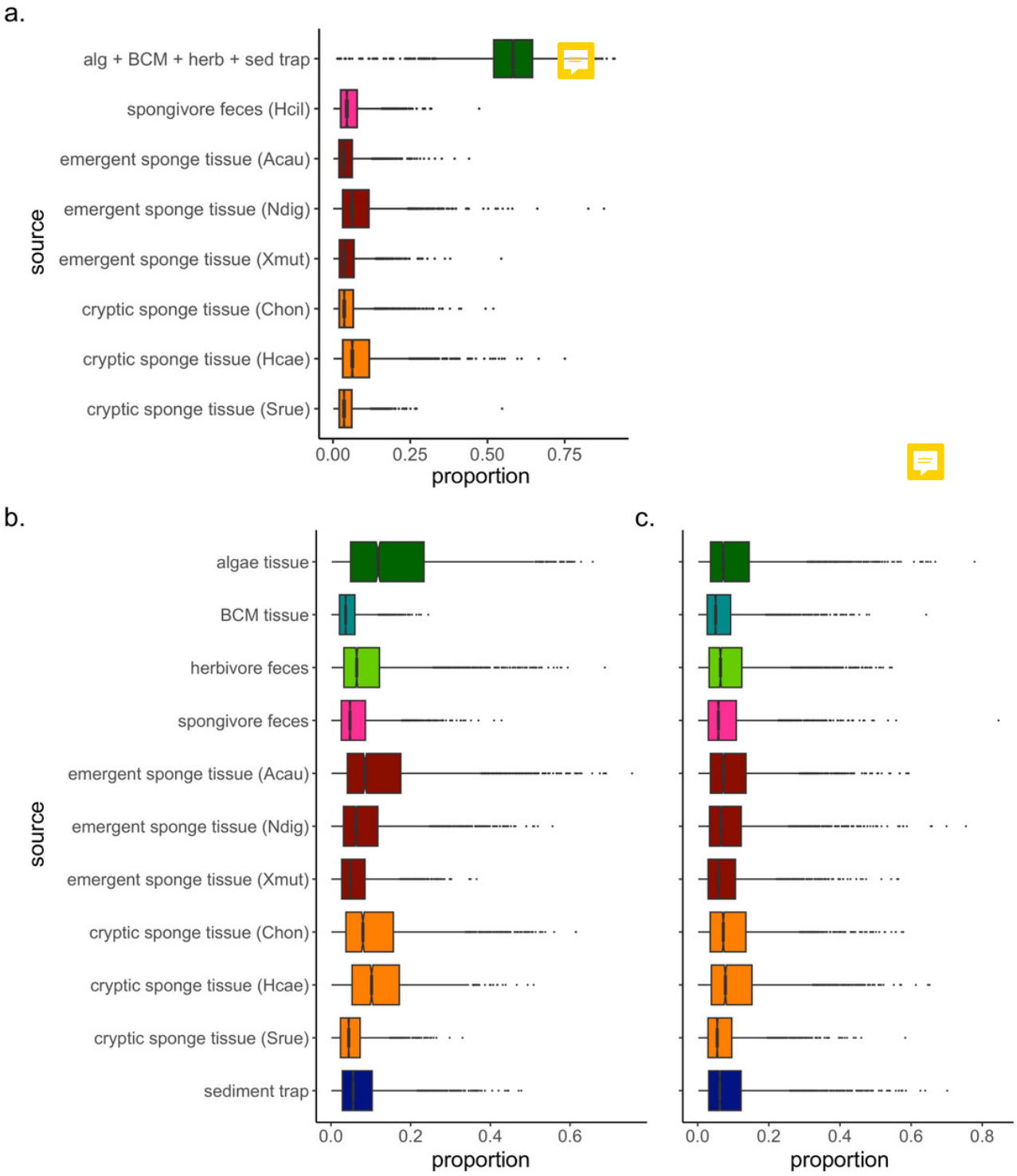
a.
alg + BCM + herb + sed trap
spongivore feces (Hcil)
emergent sponge tissue (Acau)
emergent sponge tissue (Ndig)
emergent sponge tissue (Xmut)
cryptic sponge tissue (Chon)
cryptic sponge tissue (Hcae)
cryptic sponge tissue (Srue)
source
0.00
0.25
0.50
0.75
proportion
b.
algae tissue
BCM tissue
herbivore feces
spongivore feces
emergent sponge tissue (Acau)
emergent sponge tissue (Ndig)
emergent sponge tissue (Xmut)
cryptic sponge tissue (Chon)
cryptic sponge tissue (Hcae)
cryptic sponge tissue (Srue)
sediment trap
source
0.0
0.2
0.4
0.6
proportion
c.
0.0
0.2
0.4
0.6
0.8
proportion

Figure 3

The frequencies of occurrence for all phyla in each composite sample in each year.

Number of replicates is shown in parentheses. J18 = July 2018, M19 = March 2019, EAM = detritus suctioned from epilithic algal matrix, tray = detritus sampled from trays placed under reef overhangs, sed. trap = particulates captured in sediment traps, h'vore feces = feces collected from herbivorous fishes, s'vore feces = feces collected from spongivorous fishes.

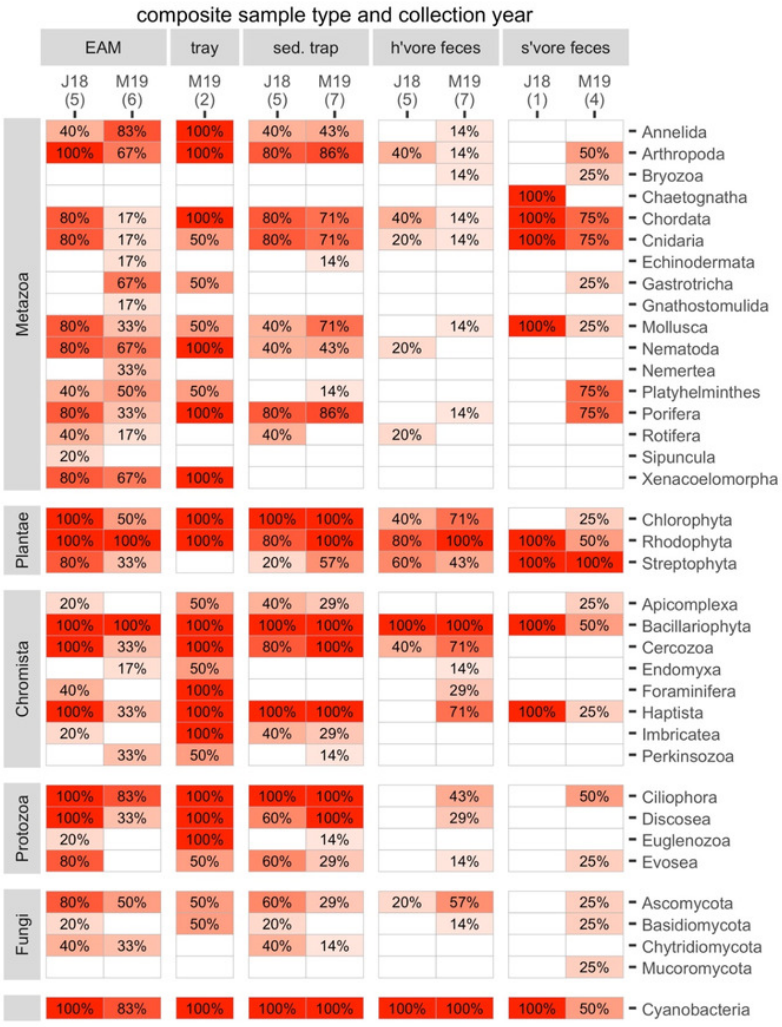
composite sample type and collection year
EAM
tray
sed. trap
h'vore feces
s'vore feces
J18 (5)
M19 (6)
M19 (2)
J18 (5)
M19 (7)
J18 (5)
M19 (7)
J18 (1)
M19 (4)
Metazoa
Annelida
Arthropoda
Bryozoa
Chaetognatha
Chordata
Cnidaria
Echinodermata
Gastrotricha
Gnathostomulida
Mollusca
Nematoda
Nemertea
Platyhelminthes
Porifera
Rotifera
Sipuncula
Xenacoelomorpha
Plantae
Chlorophyta
Rhodophyta
Streptophyta
Chromista
Apicomplexa
Bacillariophyta
Cercozoa
Endomyxa
Foraminifera
Haptista
Imbricatea
Perkinsozoa
Protozoa
Ciliophora
Discosea
Euglenozoa
Evosea
Fungi
Ascomycota
Basidiomycota
Chytridiomycota
Mucoromycota
Cyanobacteria

Figure 4

The frequencies of occurrence in composite sample types for the 15 most abundant algae and non-sponge metazoans, and all 36 identified sponge taxa.

Number of replicates is shown in parentheses. J18 = July 2018, M19 = March 2019, EAM = detritus suctioned from epilithic algal matrix, tray = detritus sampled from trays placed under reef overhangs, sed. trap = particulates captured in sediment traps, h'vore feces = feces collected from herbivorous fishes, s'vore feces = feces collected from spongivorous fishes. Classification includes phylum (P), class (C), order (O), family (F), genus (G), and species (S), where applicable. See Table S6 and Table S7 for frequencies of all algae and metazoa taxa, respectively.

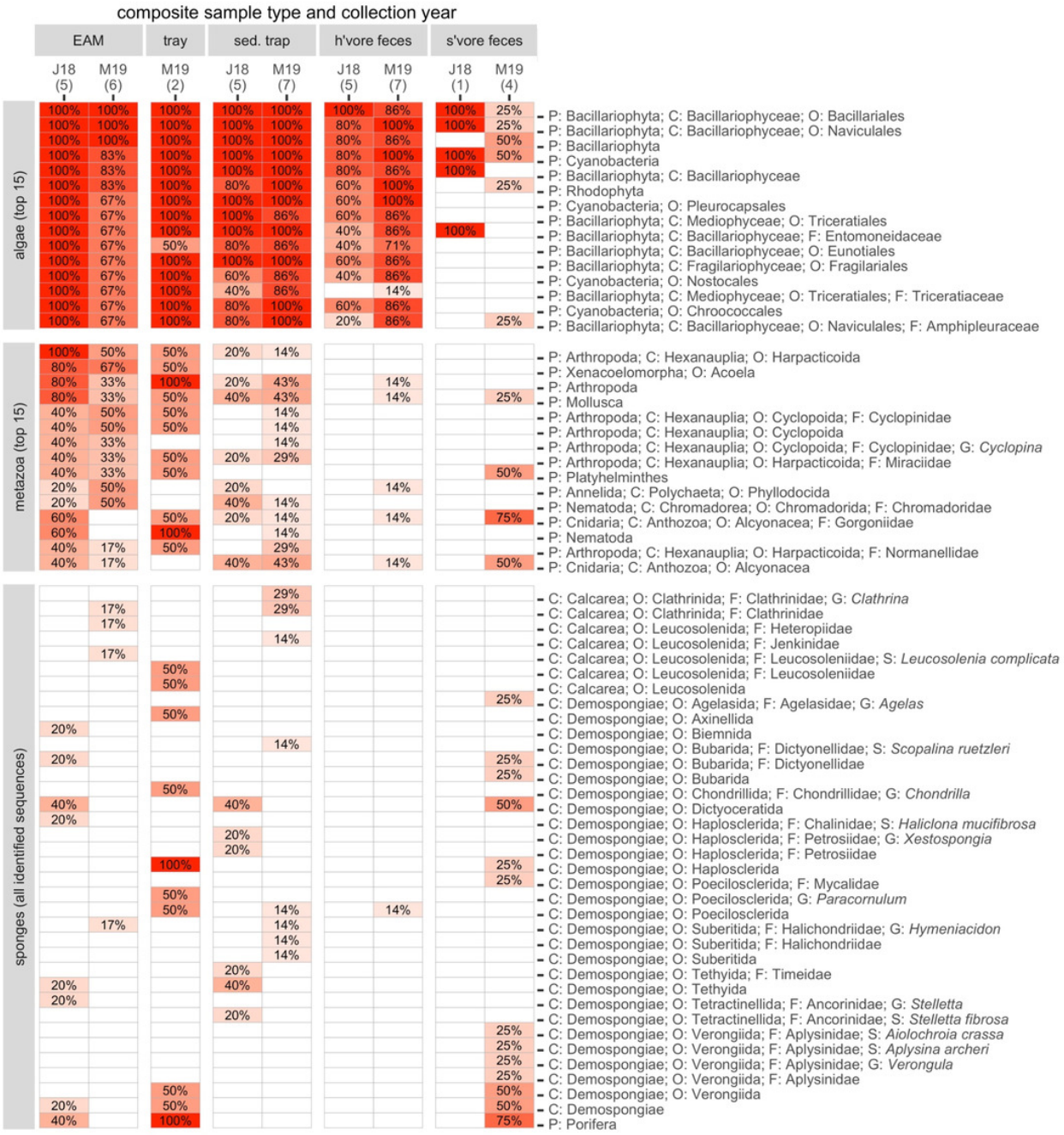
composite sample type and collection year
EAM
tray
sed. trap
h'vore feces
s'vore feces
J18 (5)
M19 (6)
M19 (2)
J18 (5)
M19 (7)
J18 (5)
M19 (7)
J18 (1)
M19 (4)
algae (top 15)
metazoa (top 15)
sponges (all identified sequences)
P: Bacillariophyta; C: Bacillariophyceae; O: Bacillariales
P: Bacillariophyta; C: Bacillariophyceae; O: Naviculales
P: Bacillariophyta
P: Cyanobacteria
P: Bacillariophyta; C: Bacillariophyceae
P: Rhodophyta
P: Cyanobacteria; O: Pleurocapsales
P: Bacillariophyta; C: Mediophyceae; O: Triceratiales
P: Bacillariophyta; C: Bacillariophyceae; F: Entomoneidaceae
P: Bacillariophyta; C: Bacillariophyceae; O: Eunotiales
P: Bacillariophyta; C: Fragilariophyceae; O: Fragilariales
P: Cyanobacteria; O: Nostocales
P: Bacillariophyta; C: Mediophyceae; O: Triceratiales; F: Triceratiaceae
P: Cyanobacteria; O: Chroococcales
P: Bacillariophyta; C: Bacillariophyceae; O: Naviculales; F: Amphipleuraceae
P: Arthropoda; C: Hexanauplia; O: Harpacticoida
P: Xenacoelomorpha; O: Acoela
P: Arthropoda
P: Mollusca
P: Arthropoda; C: Hexanauplia; O: Cyclopoida; F: Cyclopinidae
P: Arthropoda; C: Hexanauplia; O: Cyclopoida
P: Arthropoda; C: Hexanauplia; O: Cyclopoida; F: Cyclopinidae; G: Cyclopina
P: Arthropoda; C: Hexanauplia; O: Harpacticoida; F: Miraciidae
P: Platyhelminthes
P: Annelida; C: Polychaeta; O: Phyllodocida
P: Nematoda; C: Chromadorea; O: Chromadorida; F: Chromadoridae
P: Cnidaria; C: Anthozoa; O: Alcyonacea; F: Gorgoniidae
P: Nematoda
P: Arthropoda; C: Hexanauplia; O: Harpacticoida; F: Normanellidae
P: Cnidaria; C: Anthozoa; O: Alcyonacea
C: Calcarea; O: Clathrinida; F: Clathrinidae; G: Clathrina
C: Calcarea; O: Clathrinida; F: Clathrinidae
C: Calcarea; O: Leucosolenida; F: Heteropiidae
C: Calcarea; O: Leucosolenida; F: Jenkinidae
C: Calcarea; O: Leucosolenida; F: Leucosoleniidae; S: Leucosolenia complicata
C: Calcarea; O: Leucosolenida; F: Leucosoleniidae
C: Calcarea; O: Leucosolenida
C: Demospongiae; O: Agelasida; F: Agelasidae; G: Agelas
C: Demospongiae; O: Axinellida
C: Demospongiae; O: Biemnida
C: Demospongiae; O: Bubarida; F: Dictyonellidae; S: Scopalina ruetzleri
C: Demospongiae; O: Bubarida; F: Dictyonellidae
C: Demospongiae; O: Bubarida
C: Demospongiae; O: Chondrillida; F: Chondrillidae; G: Chondrilla
C: Demospongiae; O: Dictyoceratida
C: Demospongiae; O: Haplosclerida; F: Chalinidae; S: Haliclona mucifibrosa
C: Demospongiae; O: Haplosclerida; F: Petrosiidae; G: Xestospongia
C: Demospongiae; O: Haplosclerida; F: Petrosiidae
C: Demospongiae; O: Haplosclerida
C: Demospongiae; O: Poecilosclerida; F: Mycalidae
C: Demospongiae; O: Poecilosclerida; G: Paracornulum
C: Demospongiae; O: Poecilosclerida
C: Demospongiae; O: Suberitida; F: Halichondriidae; G: Hymeniacidon
C: Demospongiae; O: Suberitida; F: Halichondriidae
C: Demospongiae; O: Suberitida
C: Demospongiae; O: Tethyida; F: Timeidae
C: Demospongiae; O: Tethyida
C: Demospongiae; O: Tetractinellida; F: Ancorinidae; G: Stelletta
C: Demospongiae; O: Tetractinellida; F: Ancorinidae; S: Stelletta fibrosa
C: Demospongiae; O: Verongiida; F: Aplysinidae; S: Aiolochroia crassa
C: Demospongiae; O: Verongiida; F: Aplysinidae; S: Aplysina archeri
C: Demospongiae; O: Verongiida; F: Aplysinidae; G: Verongula
C: Demospongiae; O: Verongiida; F: Aplysinidae
C: Demospongiae; O: Verongiida
C: Demospongiae
P: Porifera

Table 1(on next page)

Number of replicates of detritus and detritus sources collected in July 2018 and March 2019 and analyzed using stable isotope analyses (n_{SIA}) and genetic sequencing (n_{seq}).

Composite samples are indicated in bold.

1

category	sample type	species	July 2018		March 2019	
			n_{SIA}	n_{seq}	n_{SIA}	n_{seq}
detritus	**EAM**	total	5	5	11	6
	tray	total	0	0	3	2
source	algae tissue	*Dictyota* sp.	5	5	5	0
		Halimeda sp.	0	0	3	0
		Lobophora variegata	5	5	6	0
		total	10	10	14	0
	BCM tissue	total	3	3	5	0
	herbivore feces	*Acanthurus bahianus*	3	3	4	6
		Acanthurus coeruleus	2	2	1	1
		total	5	5	5	7
	spongivore feces	*Holacanthus ciliaris*	1	1	1	2
		Pomacanthus paru	0	0	2	2
		total	1	1	3	4
	emergent sponge tissue	*Aplysina cauliformis*	10	0	10	0
		Niphates digitalis	8	0	10	0
		Xestospongia muta	10	5	10	0
		total	28	5	30	0
	cryptic sponge tissue	*Chondrilla* sp.	2	2	3	0
		Halisarca caerulea	3	3	4	0
		Scopalina ruetzleri	3	3	5	0
		total	8	8	12	0
	sediment trap	total	5	5	14	7

2